Arch. Mech., 32, 5, pp. 723-739, Warszawa 1980

Some fundamental aspects of laboratory simulation of snow or sand drifts near obstacles

J. de KRASIŃSKI and T. SZUSTER (CALGARY)

SAND or snow drift formation in the vicinity of obstacles plays an important role in building projects in high mountains, desert and arctic areas. The simulation of these phenomena in a water flume in the laboratory has many practical advantages and, although this technique has been used, the similarity aspects have not been adequately developed. Also the interparticle forces in the case of snow play an important role which is not yet fully understood. The paper deals with the fundamental similarity parameters required to reproduce these phenomena in the laboratory, using water as the working fluid and appropriate granulated solids. It appears from this study that a modified Froude scaling should give adequate results if properly applied. The similarity achieved by these means is, strictly speaking, a pseudo-similarity, the essentials of which are developed and critically examined. Some experimental methods have been proposed to simulate and to measure the attractive forces between the grains.

Tworzenie się zasp śnieżnych i wydm piaszczystych w pobliżu przeszkód gra ważną rolę w projektowaniu konstrukcji wznoszonych w wysokich górach, na terenach arktycznych lub pustynnych. Symulacja tych zjawisk w laboratoryjnych kanałach wodnych ma wiele zalet praktycznych i, mimo iż technika ta była już stosowana, nie zostały dotąd dostatecznie opracowane odpowiednie prawa podobieństwa. Ważną rolę grają również w przypadku śniegu oddziaływania międzycząsteczkowe, które nie zostały dotąd w pełni wyjaśnione. W pracy zajęto się podstawowymi prawami podobieństwa koniecznymi dla odtworzenia tych zjawisk w laboratorium przy użyciu wody jako cieczy roboczej i odpowiednio rozdrobnionych materiałów sypkich. Okazuje się, że zmodyfikowane prawo Froude'a powinno prowadzić do poprawnych wyników. Osiągnięte w ten sposób podobieństwo jest, mówiąc ściśle, pseudopodobieństwem; w pracy przedstawiono i krytycznie przeanalizowano jego własności. Zaproponowano pewne metody doświadczalnego symulowania i mierzenia siły oddziaływania wzajemnego między ziarnami ośrodka sypkiego.

Образование снежных сугробов и песчаных дюм вблизи преград играет важную роль в проектировании конструкций, восдвигаемых в высоких горах, в арктических или пустынных местностях. Имитация этих явлений в лабораторных водных каналах имеет много практических достоинств и несмотря на факт, что эта техника уже применялась до сих пор не были достатчно разработаны соответствующие законы подобия. Важную роль играют тоже, в случае снега, межмолекулярные взаимодействия, которые до сих пор не вполне выяснены. В работе занимаются основными законами подобия для отображения этих явлений в лаборатории при использовании воды, как рабочей жидкости и соответственно раздребленных сыпучих материалов. Оказывается, что модифицированный закон Фруда должен привести к правильным результатам. Достигнутое таким образом подобие является, говоря точно, псевдоподобием; в работе представлены и критически проанализированы его свойства. Предложены некоторые методы экспериментальной имитации и измерения силы взаимодействия между зернами сыпучей среды.

Nomenclature

A area,
C_D drag coefficient,
C nondimensional force cofficient,

D drag,
F force,
f force per unit mass,
g acceleration due to gravity,
H height of the obstacle,
K circulation,
L lift,
L size of the obstacle (prototype model),
l size of the grain (prototype and model),
m mass,
Re Reynolds number,
R radius of curvature,
s path,
T time,
U typical horizontal velocity,
U^* shear velocity,
V velocity,
X, Y horizontal and vertical components,
z_0 roughness height.

Greek

α $\frac{\varrho_w}{d_s}$,
γ density of solid,
θ angle,
δ relative apparent mass added to the grain moving in the air,
δ_u boundary layer thickness,
Δ relative apparent mass added to the grain moving in water,
Λ linear macro-scale of obstacle $= L_p/L_m$,
λ linear micro-scale of the grain $= l_p/l_m$,
ζ ratio of $\frac{U_1}{U^*}$,
Π dynamical parameter of similarity,
ψ path angle,
ϕ a measure of forces acting on the grain,
ω angular velocity,
ϱ density of the fluid (water or air).

Subscripts

a air,
c cohesive,
cr critical,
h hydrodynamical
f fluid,
g gravitational,
i floating variable,
m model,
o absence of cohesive forces,
p prototype,
r relative,
s solid,
sd sand,
sn snow,

t terminal,
w water,
x in x direction,
y in y direction,
U^* referring to "friction velocity".

1. Introduction

DUE TO THE DEVELOPMENT of polar and desert regions in the quest of energy sources, the formation of snow and sand drifts on the ground near structures exposed to the wind presents a serious problem to the engineer. There are many advantages in simulating these phenomena in the laboratory using water as fluid and adequate solid particles as sediment. This is self-evident in the case of snow. If air and snow were used in a wind tunnel, even the substitution of snow with, say, borax crystals presents serious problems, like the collection of it after the test, contamination of the laboratory, etc. Similar arguments can be put forward in the case of sand.

Water flumes are comparatively cheap to build; their energy consumption is very small and usually they are provided with a tank to collect sediment. Tests of this type for snow drift simulation round obstacles have been done sporadically using Froude scaling but the similarity principles do not seem to have been studied adequately [7, 8]. Strictly speaking, the simulation of snow drifting phenomena in a water flume is a pseudo similarity. The main point of this study is to develop the rules of such a simulation and show how valid they are when compared to more stringent similarity concepts. This study can also be applied to sand drift formation around obstacles. Some experimental methods are also discussed about relating the cohesive forces between particles on the ground and their assessment in nature and in the laboratory.

2. Physical considerations

A solid particle falling in uniform wind has gravitational and aerodynamic forces acting on it. If strict geometrical scaling were applied reducing the size of the particle and of the model representing the obstacle on the ground, it could be shown that even if Reynolds effects were absent, the ratio of the two forces would change and the principle of the similarity would be violated. This would be so even if it were physically possible to reduce the size of, say a snow-flake in the typical ratio of about 500:1. From these and similar approaches it appears that if any progress is to be made, some other ways should be studied which would fulfill basic similarity concepts at the expense of strict ruling. This brings the notion of macro- and micro-scale modelling.

An obstacle with its typical dimension, L, is reduced in the laboratory by the geometrical scale factor $\Lambda = \frac{L_p}{L_m}$, where the subscripts p and m refer to prototype and model, respectively. The scale factor Λ is understood as macro-scale reduction. The solid particle, on the other hand with typical dimension, l, may be reduced by another scale factor $\lambda = \frac{l_p}{l_m}$

which refers to the micro-scale. If $L \gg l$, there is no serious objection to such a violation of the similarity principle. It will be shown that if the density of the fluid changes by an order of magnitude for the case of the model and the micro- and macro-scale concepts are accepted, then fundamental similarity parameters will be equal between the model and the prototype under some restricting conditions.

The similarity between the fields of flow in the vicinity of an obstacle, where the streamline patterns are criss-crossed by innumerable paths of solid particles, is somewhat reminiscent of the similarity of supersonic flow fields with the streamline patterns criss-crossed by wavelets generated by the flow. The kinematic and dynamic similarity require that the corresponding angles between the streamlines and paths (or waves) remain the same.

The pertinent question which one should attempt to answer in this context are:

i) What are the numbers related to a reduced scale study of these phenomena.

ii) What is the optimum relation between the macro-scale Λ and the micro-scale λ.

iii) To what extent can one reduce the Reynolds number of the macro and micro field without distorting the similarity between the two phenomena.

The Reynolds number affects both the macro and the micro similarity. The macro similarity is reasonably taken into account by standard wind or water flume environmental aerodynamics techniques applied today using a thick boundary layer, properly modelled on the floor of the fluid stream [2, 3, 6] and does not need to be discussed here.

With reference to the micro similarity of the flow around the grain, the drag coefficient is a function of both the shape as well as the Reynolds number of the grain. In the free fall in a uniform stream the gravity forces and fluid drag reach quickly an equilibrium (see Fig. 1), this is true in the atmosphere as well in the laboratory. For both cases, however,

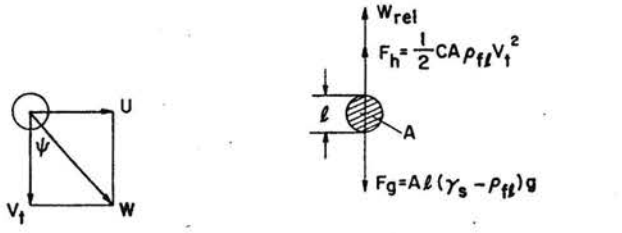

FIG. 1. A particle falling in uniform flow.

both the shape of the grain as well as its Reynolds number will be, in general, different. The particle is accelerated or decelerated due to a variety of causes (see Fig. 2). The variation of the flow field near the obstacle, the structure of the turbulence, the velocity gradient in the shear layer, etc. are the most important. The slope of the drag coefficient against the Reynolds number, i.e. $\frac{dC_D}{dR_e}$ plays an important role and not the value of the

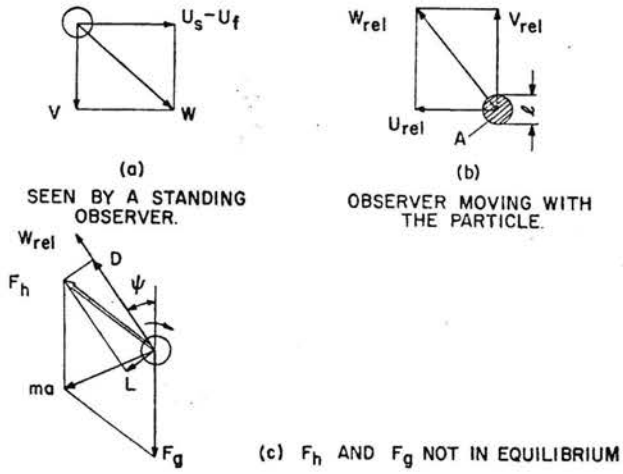

FIG. 2. A particle moving in a nonuniform flow.

drag coefficient itself. In all cases the slope by the nature of the viscous drag forces is negative, it will be only more negative or less for the model.

Moreover, the influence in view of the statistical nature of the forces, as discussed below, is not thought to be decisive.

If the flow field is otherwise similar, the velocity vectors when represented on a hodograph diagram will be oscillating around a point of equilibrium defined by the terminal velocity state. Differences between the prototype and the model due to variation of the slope of $\frac{dC_D}{dR_e}$ should not play a major role.

Another important physical reality should be kept in mind. The shape and the size of the flakes, as well as the nature of the accelerations to which the solid particles are subject in nature, have a spectral characteristic. The snow flakes, in particular, falling on the ground will not have an exactly identical crystal formation; after bouncing off the ground their shape and size varies, the cohesive forces while on the ground change from hour to hour according to temperature and humidity variations, and are modified from place to place when the crystals are crossing shaded and sun-exposed paths. Similarly, the wind energies exhibit a spectral nature. To speak in these circumstances of "exact similarity", when performing a laboratory experiment, is an exercise in pure mathematics. One can expect, however, to achieve a good overall similarity which might apply to a certain part of the spectrum displayed in reality.

3. The similarity numbers and the method of their deduction

3.1. Introduction

Similarity methods are of great value when dealing with complex phenomena which are to be modelled in a laboratory. Usually one of the two approaches is chosen: i) dimensional analysis, ii) derivation from general equations of motion. A different approach

will be made here. It was developed by W. DUNCAN [4]. He based his reasoning on Lagrange's dynamical equations. If the initial and boundary conditions are similar and the pertinent properties are respected, a generalized dynamic similarity number must hold for the model and the prototype. It is called the "generalized Froude number". If in a complex situation the number of the "typical forces per unit mass" is i, then one can form i similarity numbers Π_i where

$$\Pi_i = \left(\frac{U^2}{Lf_i}\right) = \text{const}, \tag{3.1}$$

where U is the typical velocity of the system, L its typical size and f_i the typical force per unit mass. For more details the paper [4] should be consulted. This method was chosen because of its elegance and the possibility of a simple and uniform approach to this complex problem. Other methods yield the same answers. In this approach the kinematic similarity concepts are incorporated and the law of the "corresponding times" is shown to be

$$\left(\frac{T^2 f}{L}\right)_p = \left(\frac{T^2 f}{L}\right)_m, \tag{3.2}$$

where p and m stand for prototype and the model.

It may be mentioned that out of the various interpretations of this generalized Froude number it is most meaningful to see it as the ratio between the vectorial acceleration components (normal and tangential) representative of the inertia of the system, i.e. U^2/L and the acceleration due to the "typical force" considered separately one by one, i.e. f_i (see Fig. 3). It is understood that the systems are considered similar if the paths of the

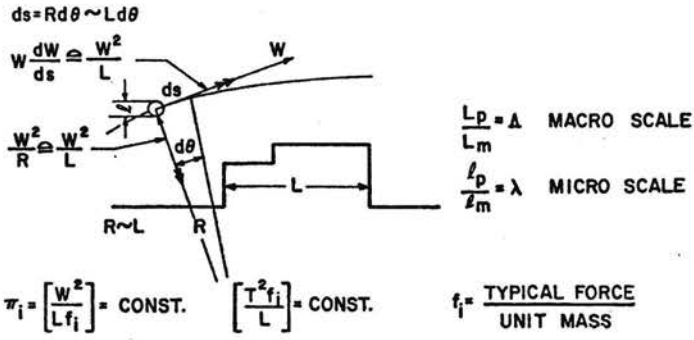

FIG. 3. An interpretation of the generalized Froude number.

particles are geometrically similar curves and the velocities at the corresponding points, as well as forces per unit mass, are in a constant ratio. It follows that the corresponding arcs of the paths and the times to describe them are also in constant ratios.

In the discussion which follows, the subscripts s and f refer to solid and fluid without specifying the nature of the solid if the fluid is water or air. If the fluid is specifically air or water, then the subscripts a or w are used. Also subscripts sd and sn are used specifically for sand and snow. In a similar way the subscript h will be used to denote the hydrodynamical force F_h as a generalized case of an aerodynamic force without making distinction if the fluid is air or water.

3.2. Kinematic similarity aspects

Two solid particles are considered in a fluid; prototype and model falling under gravitational forces, in uniform fluid flow characterized by the velocity U. After the particles reach their terminal velocity v_t, (see Fig. 1), kinematic considerations require that

$$\left(\frac{U}{v_t}\right)_p = \left(\frac{U}{v_t}\right)_m. \tag{3.3}$$

Thus if some Froude scaling is adopted and the obstacle is reduced in the laboratory by the scale factor Λ, the velocity of the stream must also be reduced. Whatever fluid and solid are used in the laboratory, it does not follow that the terminal velocity v_t of the model particle will be automatically reduced in the correct scale by simply reducing its size by the factor Λ. This reasoning brings the point that the new scale of the particle, i.e. the micro-scale, λ has to be chosen in such a way as to fulfill Eq. (3.3). Another aspect of this similarity consideration is that the path angle ψ of the solid particle must be the same at the corresponding points for the prototype and the model.

If the dynamic similarity is fulfilled, then in nonuniform flow the corresponding paths of the solid particles should also have the same inclination at the corresponding points (Figs. 1 and 2).

3.3. Similarity numbers for hydrodynamical and gravitational forces. Velocity scaling laws

Typical forces acting on the particle are the hydrodynamical, gravitational and buoyant forces. As gravity and buoyancy are of the same nature, yet act in opposite direction, the term gravitational will be used to denote the gravitational force

$$F_g = (\gamma_s - \varrho_f) g A l, \tag{3.4}$$

where γ_s and ϱ_f represent the densities of the solid fluid, respectively. l and A are the typical particle size and cross section area and g the acceleration due to gravity. The hydrodynamical force

$$F_h = \frac{1}{2} C A \varrho_f V_r^2, \tag{3.5}$$

where C is the hydrodynamical force coefficient, and V_r is the relative velocity between the particle and the fluid. The force F_h should not be understood as drag only because in general it has drag and lift components parallel and normal to the velocity vector V_r, respectively (see Fig. 2). The lift component occurs when the particle is not symmetrical, also when it rotates or crosses a velocity gradient field in the fluid.

Let us assume a macro scale of the model of the obstacle such that

$$\frac{L_p}{L_m} = \Lambda \tag{3.6}$$

and the micro scale of the solid particle

$$\frac{l_p}{l_m} = \lambda \tag{3.7}$$

so chosen that Eq. (3.3) is true. Then two parameters of dynamical similarity Π_g and Π_h can be introduced which, for the prototype and the model, give

$$(\Pi_g)_p = (\Pi_g)_m = \text{const}, \qquad (\Pi_h)_p = (\Pi_h)_m = \text{const}. \tag{3.8}$$

The gravity and hydrodynamical forces are considered as typical

$$\left(\frac{V^2}{Lf_g}\right)_p = \left(\frac{V^2}{Lf_g}\right)_m = \text{const}, \qquad \left(\frac{V^2}{Lf_h}\right)_p = \left(\frac{V^2}{Lf_h}\right)_m = \text{const}. \tag{3.9}$$

To determine f_g and f_h the mass of the particle must be known as f is the force per unit mass. A solid particle moving through fluid entrains a certain amount of it which is a fraction of its own mass, called apparent or virtual. Let this fraction be δ for the air and Δ for the water when considering prototype and model conditions of, say, snow and sand, respectively. Taking this into consideration

$$f_{gp} = \frac{A_p l_p(\gamma_{sn}-\varrho_a)g}{A_p l_p \gamma_{sn}(1+\delta)} = \frac{g}{1+\delta}\left(1-\frac{\varrho_a}{\gamma_{sn}}\right), \qquad f_{gm} = \frac{A_m l_m(\gamma_{sd}-\varrho_w)}{A_m l_m \gamma_{sd}(1+\Delta)} = \frac{g}{1+\Delta}\left(1-\frac{\varrho_w}{\gamma_{sd}}\right), \tag{3.10}$$

and their ratio

$$\frac{(f_g)_p}{(f_g)_m} = \frac{(1+\Delta)\left(1-\frac{\varrho_a}{\gamma_{sn}}\right)}{(1+\delta)\left(1-\frac{\varrho_w}{\gamma_{sd}}\right)}. \tag{3.11}$$

Similarly, for the hydrodynamical force in air or water

$$(f_h)_p = \frac{1}{2}(C)_p \frac{(V_r^2)_p \varrho_a}{l_p \gamma_{sn}(1+\delta)}, \qquad (f_h)_m = \frac{1}{2}(C)_m \frac{(V_r^2)_m \varrho_w}{l_m \gamma_{sd}(1+\Delta)}, \tag{3.12}$$

and their ratio

$$\frac{(f_h)_p}{(f_h)_m} = \frac{(C)_p (V_r^2)_p}{(C)_m (V_r^2)_m} \frac{\varrho_a}{\varrho_w} \frac{\gamma_{sd}}{\gamma_{sn}} \frac{l_m}{l_p} \frac{1+\Delta}{1+\delta}. \tag{3.13}$$

It may be observed that the mass of air entrained by the solid particle will be, in general, negligible compared to the mass of the particle; thus δ may be neglected. It is not so in the case of a solid particle in water where for silica sands Δ is of the order of 0.1 to 0.2 [1,5].

To proceed further with the development of Eqs. (3.9)–(3.12), equilibrium conditions of a free falling particle must ne considered, which means equilibrium between the hydrodynamic force F_h and gravitational (including buoyancy) force F_g.

Equilibrium for the prototype and model, respectively, require:

$$\left(\frac{1}{2} CA\varrho_a V_t^2\right)_p = [Al(\gamma_{sn}-\varrho_a)g]_p,$$

$$\left(\frac{1}{2} CA\varrho_w V_t^2\right)_m = [Al(\gamma_{sd}-\varrho_w)g]_m), \tag{3.14}$$

$$\frac{(C)_p}{(C)_m} = \frac{l_p(V_t^2)_m \frac{\gamma_{sn}}{\varrho_a} - 1}{(V_t^2)_p \frac{\gamma_{sd}}{\varrho_w} - 1}.$$

It is readily seen that the shape of the solid particle in the laboratory is of no importance as it is included in the force coefficient C. By using calibrated sieves and, say, silica sands in the water (see Fig. 6), a grain size can be found for any chosen macro-scale model scale in such a way that the kinematic conditions expressed in Eq. (3.3) are fulfilled.

Substituting Eq. (3.14) into Eq. (3.13) one obtains as expected that

$$\frac{(f_h)_p}{(f_h)_m} = \frac{(f_g)_p}{(f_g)_m} = \frac{(1+\Delta)1-\left(\frac{\varrho_a}{\gamma_{sn}}\right)}{(1+\delta)\left(1-\frac{\varrho_w}{\gamma_{sd}}\right)}, \tag{3.15}$$

which means that the ratio of hydrodynamic forces per unit mass on the grain for the prototype and the model is identical to the ratio of gravitational ones.

For a certain grain size which fulfills the kinematic condition expressed in Eq. (3.3)

$$V_t \sim V_r \sim U. \tag{3.16}$$

It also follows from Eq. (3.1) that

$$\frac{U_p^2}{U_m^2} = \frac{L_p}{L_m}\frac{f_{tp}}{f_{tm}} = \Lambda\frac{(f_t)_p}{(f_t)_m},$$

in this case

$$\frac{(f_t)_p}{(f_t)_m} = \frac{(f_g)_p}{(f_g)_m} = \frac{(f_h)_p}{(f_h)_m} = \frac{(1+\Delta)\left(1-\frac{\varrho_a}{\gamma_{sn}}\right)}{(1+\delta)\left(1-\frac{\varrho_w}{\gamma_{sd}}\right)} = \frac{(1+\Delta)(\gamma_{sn}-\varrho_a)\gamma_{sd}}{(1+\delta)(\gamma_{sd}-\varrho_w)\gamma_{sn}}. \tag{3.17}$$

The proposed velocity scaling law is a modified Froude scaling in the form

$$\frac{U_p}{U_m} = \frac{(V_t)_p}{(V_t)_m} = \sqrt{\Lambda}\sqrt{\frac{(1+\Delta)(\gamma_{sn}-\varrho_a)\gamma_{sd}}{(1+\delta)(\gamma_{sd}-\delta_w)\gamma_{sn}}} \tag{3.18}$$

in which δ can be usually ignored but not the apparent mass added to the grain in the water expressed by Δ. As the ratio ϱ_a/γ_{sn} is also small, a simple form can be used taking $\varrho_w/\gamma_{sd} = \alpha$

$$\frac{U_p}{U_m} = \frac{(V_t)_p}{(V_t)_m} = \sqrt{\Lambda}\sqrt{\frac{1+\Delta}{1-\alpha}}. \tag{3.19}$$

This ratio is plotted in Fig. 4 for silica sands and other solids.

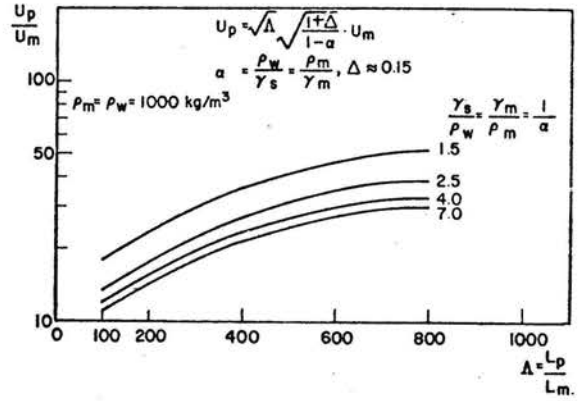

FIG. 4. The velocity scaling law.

The following observations should be made:

i) The grain size does not enter explicitly in the expression but it is implicitly included by such a choice that the kinematic similarity, Eq. (3.3), is respected (see also (*V*) below).

ii) The choice of L as typical length of the macro similarity of the flow field around the obstacle can be justified on physical grounds provided the grain $l \ll L$. It would be inadmissible, however, to reduce the size of the model to such an extent that $l = [0]L$.

iii) The law of the corresponding times (Eq. (3.2)) means that

$$\frac{T_p}{T_m} = \sqrt{\Lambda}\sqrt{\frac{1-\alpha}{1+\Delta}} \tag{3.20}$$

in which the typical time T indicates the time required to cross the typical length L of the macro field and this is more important than crossing the grain of the size l, for which the time scale is distorted.

iv) Although for illustration purposes snow in air and sand in water were given as an example, sand in air and another appropriate solid or also sandin water may be used.

v) Typical terminal velocities of silica sands in water against the grain size are plotted in Fig. 6 and give an indication of the choice of the macro scale.

3.4. Lift due to rotation. Magnus effect

A solid particle after bouncing off the ground or subject to a strong velocity gradient will begin to rotate. Tests on macro models made in this laboratory and computer simulation indicate that a great part of the so-called "meandering" phenomena of particles very close to the ground observed in sediment transport studies [11] are due to particle rotation with its associated lift force [1]. Assuming that

$$\text{Lift} \sim \varrho V K l,$$

where K is the circulation and taking $K \sim \frac{l^2}{\omega}$, where ω is the angular velocity of the particle, one obtains $K \sim Ul$. It follows that for the prototype and the model

$$\frac{(\text{Lift})_p}{(\text{Lift})_m} = \frac{\varrho_p}{\varrho_m}\frac{U_p^2}{U_m^2}\frac{l_p^2}{l_m^2}. \tag{3.21}$$

The ratios of hydrodynamical to the gravitational forces have been discussed already (Sect (3.3)). It suffices to consider the ratio of the lift due to rotation to the gravitational force only. For similarity

$$\left(\frac{\text{Lift}}{F_g}\right)_p = \left(\frac{\text{Lift}}{F_g}\right)_m, \tag{3.22}$$

where

$$F_g \sim l^3(\gamma_s - \varrho_f)\, g.$$

Taking the lift ratios from Eq. (3.21), it follows that

$$\frac{\varrho_a}{\varrho_w}\frac{l_m}{l_p}\left(\frac{\gamma_{sd}-\varrho_w}{\gamma_{sn}-\delta_a}\right)\frac{U_p^2}{U_m^2} = 1. \tag{3.23}$$

The ratio of the velocities is determined by the scaling law; eliminating it using Eq. (3.18), one gets

$$\frac{\Lambda}{\lambda}\frac{\varrho_a}{\varrho_w}\frac{\gamma_{sd}}{\gamma_{sn}}\frac{(1+\Lambda)}{(1+\delta)} = 1; \tag{3.24}$$

neglecting δ, it appears that the best size of the grains is

$$\lambda \simeq \Lambda\left(\frac{\varrho_a}{\varrho_w}\right)\frac{\gamma_{sd}}{\gamma_{sn}}(1+\Lambda) \simeq \Lambda\frac{|1+\Lambda}{\alpha}\frac{\varrho_a}{\gamma_{sn}}. \tag{3.25}$$

Although the choice of the grain is determined from the terminal velocity tests, its optimum size should be related to the macro scale of the model through Eq. (3.25). This relation is very similar to the one developed in Sect. 3.6.1 and is plotted in Fig. 5. It is interesting to note that taking the macro scale $\Lambda \simeq 500$, one obtains for standard silica sands in the water $\lambda \simeq 17$, which is the right order of magnitude between the snow flake and the sand grain. If the formation of sand drifts near obstacles in the air is to be simulated in water, then the solid density ratio in Eq. (3.25) would be unity and for a macro scale of $\Lambda = 500$, $\lambda \simeq 0.7$, i.e. a larger grain should be used than in nature, always provided that the kinematic relation (Eq. (3.3)) is fulfilled. More details are given in [9].

3.5. The effects of roughness

The usual scaling procedure in environmental aerodynamics follows JENSEN'S rule [6] which assumes a logarithmic velocity profile. It requires for the prototype and the model that

$$\frac{(\delta_u)_p}{(\delta_u)_m} = \frac{(z_0)_p}{(z_0)_m} = \frac{(H)_p}{(H)_m} = \Lambda, \tag{3.26}$$

where δ_u is the velocity boundary layer height, z_0 is the roughness height, and H is the height of the obstacle or building [2, 3, 6].

Following this rule one would like also to have this ratio respected for the prototype and the model grain size. The previous discussion has shown that this is not so and the grain size ratio

$$\frac{l_p}{l_m} = \lambda, \quad \lambda < \Lambda$$

for most of the cases.

It is difficult to foresee how this irregularity in scaling will affect the behaviour of the grains in the close vicinity to the ground. One may comment, however, as follows:

i) The roughness height z_0 is a dynamic concept not directly related to the size of the particle but rather to the configuration of the ground as a whole, like the type of vegetation, size of grass, of undergrowth or suburban buildings. In this respect, the role played by the individual grains is small and as a rule $l < z_0$ [10], so if they are comparatively large in the laboratory, this effect will be of second order of importance.

ii) The laminar sublayer in the water flume will be, in general, rather thick because of the slowness of motion and it is not always easy to maintain the condition

$$\frac{(z_0)_p}{(z_0)_m} = \Lambda;$$

a larger z_{0m} would require larger grain particles, that is exactly the case, thus in practice some compromise may be sought.

3.6. The effect of cohesive forces

In the snow and solid transport phenomena and the formation of drifts around the obstacles, integranular forces play an important role. This role is less accentuated in drifting sands but even there small clay residues combined with variable humidity cannot be neglected. In the case of snow, the time factor affecting the crystal structure combined with variations in temperature and humidity can change the order of magnitude of cohesive forces. Their assessment in the field and in the laboratory is a very difficult task, and so is their laboratory simulation. Two cases should be distinguished related to entirely different methods of measuring such forces at different physical situations:

i) The solid particles lying on the ground are subject to hydrodynamical forces which have a shear stress and a lift component. As the shear stress in the turbulent boundary layer can be assessed by the shear velocity, which is a measurable quantity, the critical value of U^* originating motion is an indirect measure of the cohesive forces. When no cohesive forces are present, a critical minimum value of (U^*) is observed. As the cohesive forces increase, so does $(U^*)_{cr}$. Such tests can be made both in the field and in the laboratory.

ii) A sample of the material appropriately protected (sand, snow, etc.) is located on a disc (for details see [9]) along its radius. The disc has a variable velocity drive and rotates in the horizontal position. At certain angular velocity $(\omega)_{cr}$ the sample begins to break down at a particular $R = (R)_{cr}$. Repeating the tests, a reasonable average can be obtained of the product $(\omega^2 R)_{cr}$ giving some consistent information about the cohesive forces within the frame of the measuring technique. Here again the tests can be performed in the field using sand or snow crystals at appropriate atmospheric conditions and also in the laboratory where the cohesive forces should be simulated in some specified way. If the centrifuge results in the field are compatible with those produced artificially in the laboratory on cohesive granular material, then one can also consider similarity between the cohesive forces. The similarity based on the two methods is discussed below.

3.6.1. Cohesive forces similarity based on shear velocity U^*. Following the previous approach, a dynamics similarity parameter can be introduced Π_{U^*} signifying that the shear stresses due to friction velocity U^* are considered, although, as mentioned before, a hydrodynamical lift force also acts on the particle. The typical force per unit mass acting on the grain in critical conditions is

$$f_{U^*} = \frac{l^2 U_{cr}^{*2} \varrho_l}{l^3 \gamma_s} = \frac{\varrho_l}{\gamma_s} \frac{(U^{*2})_{cr}}{l}.$$

The apparent mass due to the displacement of the fluid is not taken here into consideration as the solid grain is only on the point of moving but rests on the ground. The similarity parameters for the prototype and the model

$$\Pi_{U^*} = \left(\frac{U^2}{L_{f_{U^*}}}\right) = \frac{U}{\frac{L\varrho_l (U^{*2})_{cr}}{\gamma_s l}} = \text{const}. \tag{3.27}$$

For a turbulent boundary layer

$$\left(\frac{U}{U^*}\right)_{cr} \sim \left(\frac{U_1}{U^*}\right) \sim \zeta. \tag{3.28}$$

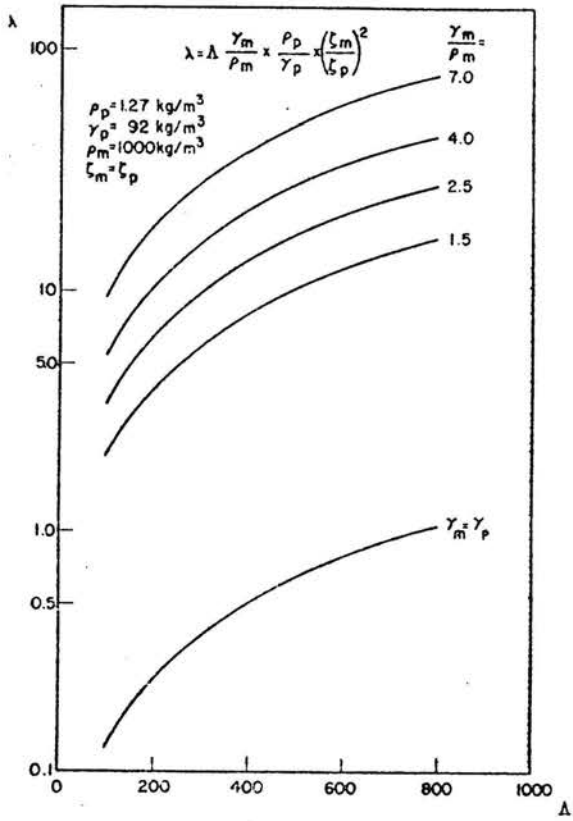

FIG. 5. Optimum grain scale against model scale.

This parameter is related to the turbulent tensile stress on the ground and may be different for the prototype and the model. Using the previous nomenclature it follows that

$$\frac{\zeta_p^2 \lambda \varrho_w \gamma_{sn}}{\zeta_m^2 \Lambda \varrho_a \gamma_{sd}} = 1 \tag{3.29}$$

and the optimum grain scale λ in terms of the model scale Λ is

$$\lambda = \Lambda \left(\frac{\zeta_m}{\zeta_p}\right)^2 \frac{\gamma_{sd}}{\gamma_{sn}} \frac{\varrho_a}{\varrho_w} \tag{3.30}$$

for the case of simulating snow with sand in the water. For simulating sand in the air (prototype) with sand in the water (model) γ_{sd}/γ_{sn} should be substituted with $\gamma_{sd}/\gamma_{sd} = 1$. This expression (3.30) is almost identical to Eq. (3.25) when $\zeta_m = \zeta_p$ except for the factor $(1+\Delta)$ and is plotted on Fig. 5.

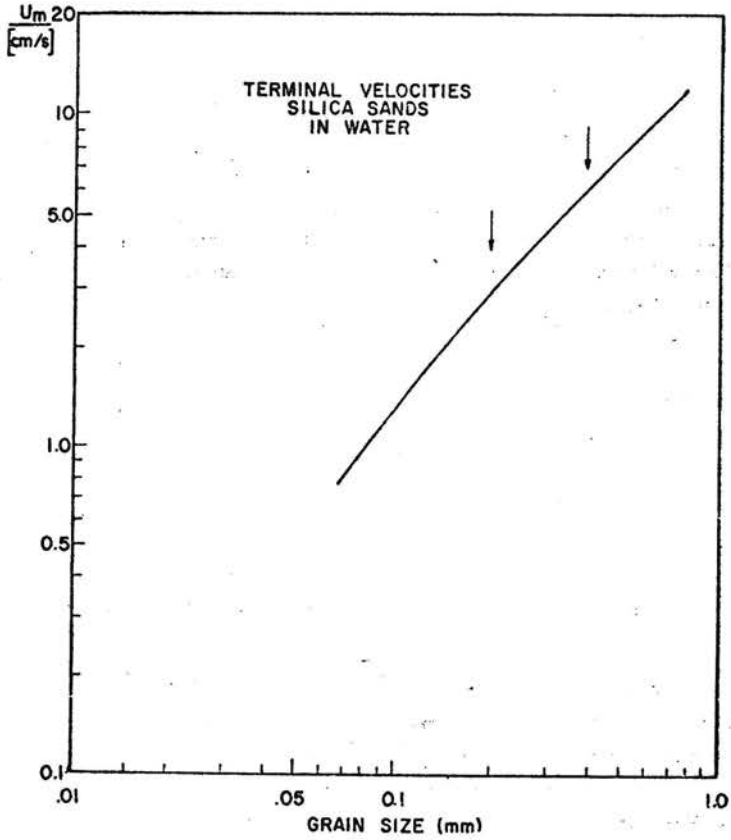

FIG. 6. Typical terminal velocities for silica sands.

The relation (3.28) also means that

$$(U_p^*)_{cr} = (U_m^*)_{cr} \left(\frac{U_p}{U_m}\right) \frac{\zeta_m}{\zeta_p}.$$

As U_p/U_m are related (Eq. (3.19)), it follows that

$$(U_p^*)_{cr} = (U_m^*)_{cr}\sqrt{\Lambda}\sqrt{\frac{1+\Delta}{1-\alpha}\frac{\zeta_m}{\zeta_p}}. \tag{3.31}$$

In view of the difficulties in meeting the principles of similarity very close to the ground, which were discussed in Sect. 3.5, it is questionable whether Eq. (3.31) can be followed with certainty even if the similarity of the cohesive forces is correct. More experiments would be needed to obtain with reasonable certainty the critical saltation velocity for the prototype using a laboratory model.

3.6.2. Cohesive forces similarity based on the measurements of centrifugal forces. In principle, the similarity can be obtained as the ratio between the horizontal and vertical forces acting on the articles when the horizontal forces are big enough to produce a movement of the granular material. If no cohesive forces act on the particles, only pure dry friction critical conditions are observed at, say, radius R_0 and angular velocity ω_0. For the tests in the air and the water the sample is enclosed in a transparent, closed tube to avoid external interference and spilling of the water. Particles in the fluid are subjected to a centrifugal head.

1) *No cohesive forces*

At the free end each particle is subject to a horizontal and vertical force component. When the horizontal component overcomes the frictional forces, it starts to move at a certain critical condition of the product $(\omega_0^2 R_0)$. The horizontal and vertical forces on each grain at the free end are

$$(F_{x0})_p = l_p^3(\gamma_s-\varrho_a)(\omega^2 R_0)_p,$$
$$(F_{y0})_p = l^3(\gamma_s-\varrho_a)g;$$

assuming

$$(\omega_0^2 R_0)_p = g(\phi_{x0})_p$$

their ratio is

$$\left(\frac{F_{x0}}{F_{y0}}\right)_p = \left(\frac{\omega_0^2 R_0}{g}\right)_p = \left(\frac{g\phi_{x0}}{g}\right)_p = \phi_{x0},$$

where ϕ_{x0} is a measure of dry friction.

Similarly, for the model in the water

$$(F_{x0})_m = l_m^3(\gamma_s-\varrho_w)(\omega_0^2 R_0)_m = l^3(\gamma_s-\varrho_o)g\phi(x_0)_m,$$
$$(F_{y0})_m = l^3(\gamma_s-\varrho_w)g$$

and again their ratio is

$$\left(\frac{F_{x0}}{F_{y0}}\right)_m = (\phi_{x0})_m.$$

For similarity conditions

$$(\phi_{x0})_p = (\phi_{x0})_m.$$

Typical values of $(\phi_{x0})_p$ for sands are 0.35 to 0.4

2) *Cohesive forces included*

With cohesive forces the measurements on the centrifuge become less meaningful. If the sample is positioned radially on a very rough surface, it will break off at a certain critical ω and radius r. These values which are a measure of the horizontal force required to break off the sample include both the shear and normal stresses due to cohesion and friction. Although the tests are repeatable and comparable in a certain apparatus of given geometry, they give only a relative information as to the intensity of the cohesion forces. One would expect as in the previous case that in the same apparatus tests on cohesive grains in water and with snow in the air should be of the same order. It may be noted that for dry spring, snow at $-5°C$ in the atmosphere gave $\left(\frac{\omega^2 R}{g}\right)_{cr} \sim 14$, an order of magnitude more than for dry sand (for more details see [9]).

3.7. Effects of the elasticity of the bed

Initial laboratory tests [9] performed on macro models in the water using stroboscopic photography indicated that the rotation of the model had a much more pronounced effect on the trajectory of the particle than the variation of the elastic characteristics of the bed. For the case of saltation on ice the restitution coefficient cannot be neglected. Usually, however, in the case of saltation of snow on snow surface or sand on sand surface, the coefficient of restitution is poor and at this point of research it appeared useless to make systematic tests on its effects.

4. Concluding remarks

A method has been proposed to simulate in the laboratory the behaviour of solid particles in the air in the vicinity of obstacles. This method can be used for any solid particles in fluids but has a particular meaning for simulating the formation of snow and sand drifts near buildings.

To achieve a kinematic similarity, it is shown that the angle of fall of the particle must be the same for the model and the prototype. This signifies for most laboratory simulation a distortion of the micro scale, i.e. of the size of the particle in the laboratory as compared to the size of the obstacle. It appears that this inconsistency is not important provided that $l \ll L$ where l is the size of the particle and L the size of the obstacle.

Methods are also developed to measure and simulate the cohesive forces between the particles on the ground which play an important role in the case of the snow.

This work is the first of a series of reports of the research programme which includes experimental techniques, a mathematical model and a computer model.

Acknowledgement

The authors gratefully acknowledge the help of Imperial Oil Ltd., Canada for their grant and the supporting staff of the Department of Mechanical Engineering of the University of Calgary in the laboratory experiments.

References

1. A. BATCHELOR, *An introduction to fluid mechanics*, Cambridge University Press, 1962.
2. J. CERMAK and V. SANDBORN, *Simulation of atmospheric motion by wind tunnel flows*, Fluid Dynamics and Diffusion Laboratory, College of Engineering, Colorado State University, Fort Collins, Colorado May 1966.
3. J. CERMAK, and S. ARYA, *Problems of atmospheric shear flows and their laboratory simulation*, Boundary Layer Meteorology, 1, 40–60, Reider Publ. Comp., Dodrecht, Holland 1970.
4. W. DUNCAN, *Physical similarity and dimensional analysis*, E. Arnold, London 1953.
5. S. ESQUINAZI, *Principles of fluid mechanics*, J. Ed. Bacon Inc., 316–319, 1968.
6. M. JENSEN, *The model law for phenomena in natural wind*, Ing. Internat. Ed., 2, 4, 121–128, 1958.
7. R. KIND, *A critical examination of requirements for model simulation of wind-induced ground drift or erosion phenomena in wind tunnels with particular emphasis on snow drifting*, NRC Laboratory Techn., Report LTR-LA-167, August 1974.
8. J. DE KRASIŃSKI and W. ANSON, *The study of snow drifts around the Canada building in Calgary*, Dept. Mech. Eng. Report, 71, October 1975.
9. J. DE KRASINSKI and T. SZUSTER, *Note on the experimental techniques used to simulate the formation of snow or sand drifts around obstacles*, Report No 154 Dept. Mech. Engg., The University of Calgary, 1979.
10. D. SLADE, *Meteorology and atomic energy*, U. S. Atomic Energy Commission, July 1968.
11. M. S. YALIN, *Mechanics of sediment transport*, Mac-Millan Pergamon Press, 1972.

DEPARTMENT OF MECHANICAL ENGINEERING
THE UNIVERSITY OF CALGARY, ALBERTA, CANADA.

Received December 3, 1979.